Functionally Graded Piezoelectric Strip with Eccentric Crack Under Anti-plane Shear

Jeong Woo Shin*
Korea Aerospace Research Institute, 45 Eoeun-Dong, YouSeong-Gu, Daejeon, 305-333, Korea
Tae-Uk Kim
Korea Aerospace Research Institute, 45 Eoeun-Dong, YouSeong-Gu, Daejeon, 305-333, Korea

In this paper, we examine the singular stresses and electric fields in a functionally graded piezoelectric ceramic strip containing an eccentric crack off the center line under anti-plane shear loading with the theory of linear piezoelectricity. It is assumed that the properties of the functionally graded piezoelectric ceramic strip vary continuously along the thickness. Fourier transforms are used to reduce the problem to the solution of two pairs of dual integral equations, which are then expressed to a Fredholm integral equation of the second kind. Numerical values on the stress intensity factor and the energy release rate are obtained.

Key Words : Functionally Graded, Piezoelectric Strip, Eccentric Crack, Stress Intensity Factor, Energy Release Rate

1. Introduction

Piezoelectric ceramic materials have recently attracted extensive attention in view of their applications to smart sensors and actuators. When piezoelectric ceramics are subjected to mechanical and electrical stresses in service, the initiation and propagation of crack may result in the failure of these materials. To prevent failure during service and to obtain the reliable service lifetime of piezoelectric components, the fracture mechanics of piezoelectric ceramics has been paid more attentions to in recent years. However, most researches examined homogeneous models and few fracture mechanics research of functionally graded piezoelectric material are presented (Li and Weng, 2002).

For the electric boundary condition on the crack surface, two controversial assumptions, permeable or impermeable, have been used by many researchers. Parton (1976), Zhang and Hak (1992) and Hao and Shen (1994) proposed a permeable crack boundary condition which assumes the continuity of electric displacement across the crack faces. Shindo et al. (1996, 1997) proposed special electric crack boundary condition and Gao and Fan (1999) proposed continuous crack boundary condition. But these two boundary conditions are similar to permeable crack boundary condition. On the contrary, Deeg (1980), Sosa (1992), Pak (1992) and Xu and Rajapakse (1999) adopted an impermeable crack boundary condition, i.e., the vanishing of normal electric displacement on the crack faces. Also, Kumar and Singh (1997) showed the validity of impermeable condition using FEM analysis. But these two boundary conditions have not been verified yet, so each researcher presented different results. Recently, Xu and Rajapakse (2001) found that the exact electric boundary conditions accounting for the medium inside the crack gaps would be reduced to the impermeable crack model when the poling direction is perpendicular to the applied electric field, so impermeable boundary condition is more suitable in this paper.

* Corresponding Author,
E-mail : jeongdal@kari.re.kr
TEL : +82-42-860-2026; **FAX** : +82-42-860-2009
Korea Aerospace Research Institute, 45 Eoeun-Dong, YouSeong-Gu, Daejeon, 305-333, Korea. (Manuscript **Received** December 20, 2002; **Revised** March 4, 2003)

In this paper, we apply the theory of linear piezoelectricity to the electroelastic problem of a finite eccentric crack off the center line in a functionally graded piezoelectric ceramic strip under anti-plane shear loading. We assume that the properties of the functionally graded piezoelectric ceramic strip vary continuously along the thickness. The impermeable crack boundary condition is adopted. Fourier transforms are used to reduce the problem to the solution of two pairs of dual integral equations, which are expressed to a Fredholm integral equation of the second kind. Numerical results for the stress intensity factor and the energy release rate are shown graphically.

2. Problem Statement and Method of Solution

Consider a functionally graded piezoelectric medium in the form of an infinitely long strip containing a finite eccentric crack off the center line subjected to the combined mechanical and electric loads as shown in Fig. 1. A set of cartesian coordinates (x, y, z) is attached to the center of the crack. The piezoelectric ceramic strip poled with z-axis occupies the region $(-\infty<x<\infty, -h_2\leq y\leq h_1, 2h=h_1+h_2)$, and is thick enough in the z-direction to allow a state of anti-plane shear. The crack is situated along the virtual interface $(-a\leq x\leq a, y=0)$, and the material properties are same on the virtual interface. Because of the assumed symmetry in geometry and loading, it is sufficient to consider the problem for $0\leq x<\infty$ only.

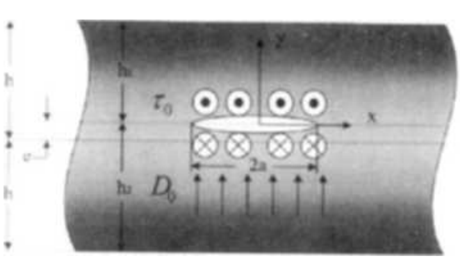

Fig. 1 A functionally graded piezoelectric ceramic strip with an eccentric crack: definition of geometry and loadings

We assume that the properties of the functionally graded piezoelectric ceramic strip vary continuously along the thickness and are simplified as follows (Erdogan, 1985),

$$c_{44}=c_{44}^0 e^{\beta y} \tag{1}$$

$$d_{11}=d_{11}^0 e^{\beta y} \tag{2}$$

$$e_{15}=e_{15}^0 e^{\beta y} \tag{3}$$

where c_{44}, d_{11} and e_{15} are the elastic modulus, the dielectric permittivity and the piezoelectric constant, respectively. c_{44}^0, d_{11}^0 and e_{15}^0 are material properties at $y=0$, and β is the non-homogeneous material constant.

The piezoelectric boundary value problem is simplified considerably if we consider only the out-of-plane displacement and the in-plane electric fields such that

$$u_{xi}=u_{yi}=0,\ u_{zi}=w_i(x, y) \tag{4}$$

$$E_{xi}=E_{xi}(x, y),\ E_{yi}=E_{yi}(x, y),\ E_{zi}=0 \tag{5}$$

where u_{ki} and $E_{ki}(k=x, y, z)$ are displacements and electric fields, respectively. Subscript $i(i=1, 2)$ stands for upper and lower regions, respectively.

In this case, the constitutive relations become

$$\sigma_{zji}(x, y)=c_{44}w_{i,j}+e_{15}\phi_{i,j} \tag{6}$$

$$D_{ji}(x, y)=e_{15}w_{i,j}-d_{11}\phi_{i,j} \tag{7}$$

where σ_{zji}, $D_{ji}(j=x, y)$ and ϕ_i are the stress components, the electric displacements and the electric potential, respectively.

Anti-plane governing equations are simplified to

$$c_{44}\nabla^2 w_i+e_{15}\nabla^2\phi_i+\beta\left(c_{44}\frac{\partial\omega_i}{\partial y}+e_{15}\frac{\partial\phi_i}{\partial y}\right)=0 \tag{8}$$

$$e_{15}\nabla^2 w_i-d_{11}\nabla^2\phi_i+\beta\left(e_{154}\frac{\partial\omega_i}{\partial y}-d_{11}\frac{\partial\phi_i}{\partial y}\right)=0 \tag{9}$$

where $\nabla^2=\partial^2/\partial x^2+\partial^2/\partial y^2$ is the two dimensional Laplace operator.

The boundary conditions are written as follows,

$$\sigma_{yzi}(x, 0)=\tau_0 \qquad (0\leq x<a) \tag{10}$$

$$w_1(x, 0^+)=w_2(x, 0^-) \qquad (a\leq x<\infty) \tag{11}$$

$$D_{yi}(x, 0) = D_0 \qquad (0 \le x < a) \tag{12}$$

$$\phi_1(x, 0^+) = \phi_2(x, 0^-) \qquad (a \le x < \infty) \tag{13}$$

$$\sigma_{yz1}(x, 0^+) = \sigma_{yz2}(x, 0^-) \qquad (a \le x < \infty) \tag{14}$$

$$D_{y1}(x, 0^+) = D_{y2}(x, 0^-) \qquad (a \le x < \infty) \tag{15}$$

$$\sigma_{yz1}(x, h_1) = \sigma_{yz2}(x, -h_2) = 0 \quad (0 \le x < \infty) \tag{16}$$

$$D_{y1}(x, h_1) = D_{y2}(x, -h_2) = 0 \quad (0 \le x < \infty) \tag{17}$$

where τ_0 and D_0 are a uniform shear stress and electric displacement, respectively.

A Fourier transform is applied to Eqs. (8) and (9), and the results are

$$w_i(x, y) = \frac{2}{\pi}\int_0^\infty \{A_{1i}(s)e^{q_1 y} + A_{2i}(s)e^{-q_2 y}\}\cos(sx)\,ds \tag{18}$$

$$\phi_i(x, y) = \frac{2}{\pi}\int_0^\infty \{B_{1i}(s)e^{q_1 y} + B_{2i}(s)e^{-q_2 y}\}\cos(sx)\,ds \tag{19}$$

where

$$q_1 = \gamma - \frac{\beta}{2},\ q_2 = \gamma + \frac{\beta}{2} \tag{20}$$

$$\gamma = \sqrt{s^2 + \frac{\beta^2}{4}} \tag{21}$$

and A_{ji}, $B_{ji}(j=1, 2)$ are the unknowns to be solved.

It is convenient to use the following definitions,

$$A_{11}(s) + A_{21}(s) - A_{12}(s) - A_{22}(s) = 2D(s) \tag{22}$$

$$B_{11}(s) + B_{21}(s) - B_{12}(s) - B_{22}(s) = 2E(s) \tag{23}$$

Using the Eqs. (14) ~ (17), (22) and (23), and the mixed boundary conditions Eqs. (10) ~ (13), we can obtain the following two simultaneous dual integral equations,

$$\begin{aligned}&\int_0^\infty sF(s)D(s)\cos(sx)\,ds\\ &= \frac{\pi}{2}\frac{1}{\mu^0}\left(\tau_0 + \frac{e_{15}^0}{d_{11}^0}D_0\right) \qquad (0 \le x < a)\end{aligned} \tag{24}$$

$$\int_0^\infty D(s)\cos(sx)\,ds = 0 \qquad (a \le x < \infty) \tag{25}$$

$$\begin{aligned}&\int_0^\infty sF(s)E(s)\cos(sx)\,ds\\ &= \frac{\pi}{2}\frac{1}{d_{11}^0}\left[\frac{e_{15}^0}{\mu^0}\left(\tau_0 + \frac{e_{15}^0}{d_{11}^0}D_0\right) - D_0\right] (0 \le x < a)\end{aligned} \tag{26}$$

$$\int_0^\infty E(s)\cos(sx)\,ds = 0 \qquad (a \le x < \infty) \tag{27}$$

where

$$F(s) = \frac{q_2}{s}\frac{2k}{k+1}\frac{(1-e^{-2\gamma h_2})(1-e^{-2\gamma h_1})}{1-e^{-4\gamma h}} \tag{28}$$

$$k = \frac{q_1}{q_2} \tag{29}$$

$$\mu^0 = c_{44}^0 + \frac{e_{15}^{02}}{d_{11}^0} \tag{30}$$

To solve the dual integral equations, we define $D(s)$ and $E(s)$ in the forms,

$$D(s) = \int_0^a \xi \Phi_1(\xi) J_0(s\xi)\,d\xi \tag{31}$$

$$E(s) = \int_0^a \xi \Phi_2(\xi) J_0(s\xi)\,d\xi \tag{32}$$

where $J_0(s\xi)$ is the zero-order Bessel function of the first kind.

Inserting the Eqs. (31) and (32) into the Eqs. (24) ~ (27), we can find that the auxiliary functions $\Phi_1(\xi)$ and $\Phi_2(\xi)$ are given by a Fredholm integral equation of the second kind in the form,

$$\begin{aligned}&\Phi_1(\xi) + \int_0^a K(\xi, \eta)\Phi_1(\eta)\,d\eta\\ &= \frac{\pi}{2}\frac{1}{\mu^0}\left(\tau_0 + \frac{e_{15}^0}{d_{11}^0}D_0\right)\end{aligned} \tag{33}$$

$$\begin{aligned}&\Phi_2(\xi) + \int_0^a K(\xi, \eta)\Phi_2(\eta)\,d\eta\\ &= \frac{\pi}{2}\frac{1}{d_{11}^0}\left[\frac{e_{15}^0}{\mu^0}\left(\tau_0 + \frac{e_{15}^0}{d_{11}^0}D_0\right) - D_0\right]\end{aligned} \tag{34}$$

where

$$K(\xi, \eta) = \eta\int_0^\infty s\{F(s) - 1\}J_0(s\eta)J_0(s\xi)\,ds \tag{35}$$

For the sake of convenience, we define the following non-dimensional quantities,

$$\eta = aH,\ \xi = a\Xi,\ s = \frac{S}{a},\ \gamma = \frac{\Gamma}{a},\ \beta = \frac{B}{a} \tag{36}$$

$$\begin{aligned}\Phi_1(\xi) &= \frac{\pi}{2}\frac{1}{\mu^0}\left(\tau_0 + \frac{e_{15}^0}{d_{11}^0}D_0\right)\frac{\Psi(\Xi)}{\sqrt{\Xi}}\\ \Phi_1(\eta) &= \frac{\pi}{2}\frac{1}{\mu^0}\left(\tau_0 + \frac{e_{15}^0}{d_{11}^0}D_0\right)\frac{\Psi(H)}{\sqrt{H}}\end{aligned} \tag{37}$$

$$\begin{aligned}\Phi_2(\xi) &= \frac{\pi}{2}\frac{1}{d_{11}^0}\left[\frac{e_{15}^0}{\mu^0}\left(\tau_0 + \frac{e_{15}^0}{d_{11}^0}D_0\right) - D_0\right]\frac{\Psi(\Xi)}{\sqrt{\Xi}}\\ \Phi_2(\eta) &= \frac{\pi}{2}\frac{1}{d_{11}^0}\left[\frac{e_{15}^0}{\mu^0}\left(\tau_0 + \frac{e_{15}^0}{d_{11}^0}D_0\right) - D_0\right]\frac{\Psi(H)}{\sqrt{H}}\end{aligned} \tag{38}$$

Substituting Eqs. (36) ~ (38) into Eqs. (33) ~ (35), we can obtain a Fredholm integral equation of the second kind in the form,

$$\Psi(\Xi)+\int_0^1 L(\Xi, H)\,\Psi(H)\,dH=\sqrt{\Xi} \qquad (39)$$

where

$$L(\Xi, H)=\sqrt{\Xi H}\int_0^\infty S\{F(s/a)-1\}J_0(SH)J_0(S\Xi)\,dS \qquad (40)$$

$$F(S/a)=\frac{Q_2}{S}\frac{2K}{K+1}\frac{(1-e^{-2\Gamma(\frac{h}{a}+\frac{e}{a})})(1-e^{-2\Gamma(\frac{h}{a}-\frac{e}{a})})}{1-e^{-4\Gamma\frac{h}{a}}} \qquad (41)$$

$$Q_1=\Gamma-\frac{B}{2},\quad Q_2=\Gamma+\frac{B}{2},\quad K=\frac{Q_1}{Q_2} \qquad (42)$$

$$\Gamma=\sqrt{S^2+\frac{B^2}{4}} \qquad (43)$$

e denotes the eccentricity.

Extending the traditional concept of stress intensity factor to other field variables, we have

$$K^T=K_{III}=\tau_0\sqrt{\pi a}\,\Psi(1) \qquad (44)$$

$$K^S=\frac{1}{\mu^0}\left(\tau_0+\frac{e_{15}^0}{d_{11}^0}D_0\right)\sqrt{\pi a}\,\Psi(1) \qquad (45)$$

$$K^D=D_0\sqrt{\pi a}\,\Psi(1) \qquad (46)$$

$$K^E=\frac{1}{d_{11}^0}\left[-\frac{e_{15}^0}{\mu^0}\left(\tau_0+\frac{e_{15}^0}{d_{11}^0}\right)+D_0\right]\sqrt{\pi a}\,\Psi(1) \qquad (47)$$

where K^T, K^S, K^D and K^E are stress intensity, strain intensity, electric displacement intensity and electric field intensity factor, respectively.

Evaluating the energy release rate G for the anti-plane case obtained by Pak (1990) on a vanishingly small contour at a crack tip, we can obtain

$$G=\frac{K^TK^S-K^DK^E}{2}=\frac{\pi a}{2}\left[\frac{1}{\mu^0}\left(\tau_0+\frac{e_{15}^0}{d_{11}^0}D_0\right)^2-\frac{D_0^2}{d_{11}^0}\right][\Psi(1)]^2 \qquad (48)$$

3. Discussions

Equation (39) is reduced to the solution (Kwon et al., 2000) for an infinite piezoelectric strip containing a central crack parallel to the strip edges by ignoring inhomogeneity and eccentricity ($\beta=0$ and $e=0$). This implies the correctness and accuracy of our results.

Table 1 Material properties of piezoelectric ceramic at $y=0$

Material Properties	Symbol	Unit	Piezoceramics
Elastic stiffness	c_{44}^0	$\times 10^{10}$ N/m^2	2.3
Piezoelectric constants	e_{15}^0	C/m^2	17.0
Permittivity	d_{11}^0	$\times 10^{-10}$ F/m	150.4
Critical energy release rate	G_{cr}	N/m	5.0

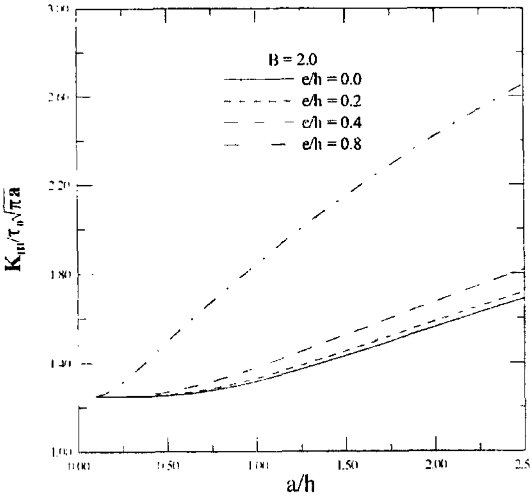

Fig. 2 Stress intensity factor $K_{III}/\tau_0\sqrt{\pi a}$ versus a/h with various values of e/h at $B=2.0$

To examine the effect of electro-mechanical interactions on the stress intensity factor and the energy release rate, we assume that piezoelectric material properties at $y=0$ are same as PZT-5H which are listed in Table 1.

Figure 2 displays the variation of the normalized stress intensity factor $K_{III}/\tau_0\sqrt{\pi a}$ versus a/h with various e/h values at $B=2.0$. Stress intensity factor (SIF) increases when the crack length and the eccentricity increase. Figure 3 shows the variation of the normalized stress intensity factor $K_{III}/\tau_0\sqrt{\pi a}$ versus a/h with various values at $e/h=0.0$. SIF increases with the increase of the crack length and non-homogeneous material constant values. The normalized energy release rate G/G_{cr} is shown in Fig. 4 and 5 for crack length of $2a=0.02$ m, $\tau_0=3.2\times 10^6$ N/m^2 and $D_0=4.8\times 10^{-3}$ C/m^2. Energy release rate (ERR) increases with the increase of the crack length, eccentricity and non-homogeneous ma-

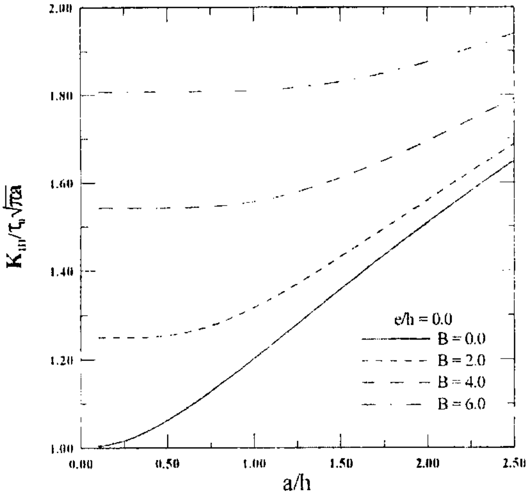

Fig. 3 Stress intensity factor $K_{III}/\tau_0\sqrt{\pi a}$ versus a/h with various values of B at $e/h=0.0$

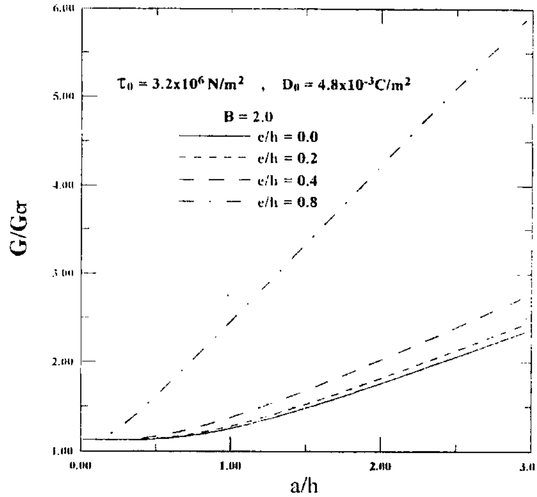

Fig. 4 Energy release rates G/G_{cr} versus a/h with various values of e/h at $B=2.0$

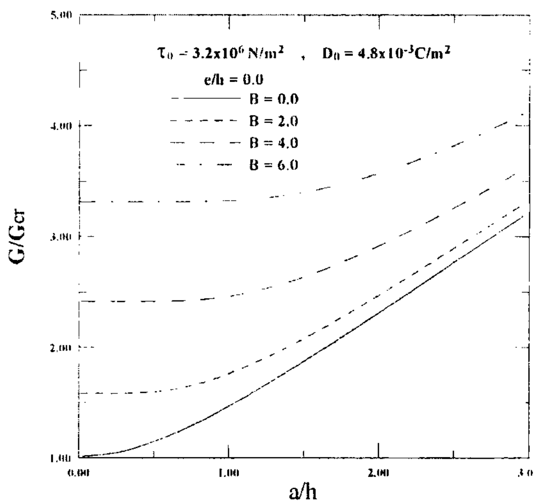

Fig. 5 Energy release rates G/G_{cr} versus a/h with various values of B at $e/h=0.0$

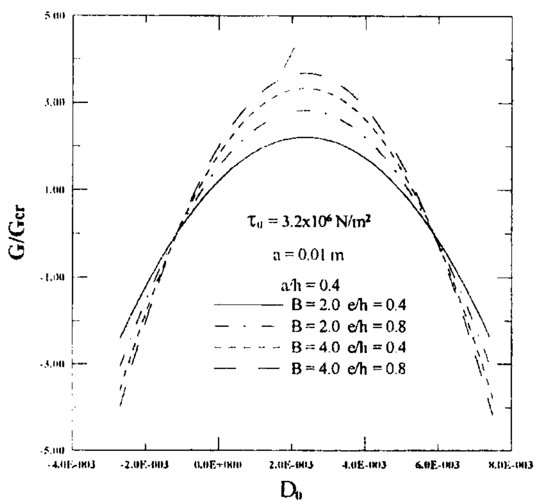

Fig. 6 Energy release rates G/G_{cr} versus D_0 with various values of B and e/h

terial constant values. Figure 6 shows the variation of the normalized energy release rate G/G_{cr} versus D_0 with various values of B and e/h. ERR increases and decreases depending on the direction and magnitude of electrical loading. And for certain electrical load, the sign of ERR can be negative. Negative value of ERR means crack retarding. This results agrees with those of Deeg (1980), Sosa (1992), Pak (1990, 1992), Xu and Rajapakse(1999) and Kwon et al. (2000).

4. Conclusions

The eccentric crack problem in a functionally graded piezoelectric ceramic strip was analyzed by the integral transform approach. The traditional concept of linear elastic fracture mechanics is extended to include the piezoelectric effects and the results are expressed in terms of the stress intensity factor and the energy release rate. The stress intensity factor and the energy release rate increase as the crack length increases and the location of crack approaches to the surface. And the stress intensity factor and the energy release rate also increase when the non-homogeneous material constant increases. Retard of crack growth occurs dependent on the direction and magnitude of electrical loading.

References

Deeg, W. F., 1980, "The Analysis of Dislocation, Crack and Inclusion Problem in Piezoelectric Solids," Ph. D. Thesis, Stanford University, Stanford, CA.

Erdogan, F., 1985, "The Crack Problem for Bonded Nonhomogeneous Materials Under Antiplane Shear Loading, " *ASME, Journal of Applied. Mechanics*, Vol. 52, pp. 823~828.

Gao, C. F. and Fan, W. X., 1999, "A General Solution for the Plane Problem in Piezoelectric Media with Collinear Crack," *International Journal of Engineering Science*, Vol. 37, pp. 347~363.

Hao, T. H. and Shen, Z. Y., 1994, "A New Electric Boundary Condition of Electric Fracture Mechanics and Its Applications," *Engineering Fracture Mechanics*, Vol. 47, pp. 793~802.

Kumar, S. and Singh, R. N., 1997, "Influence of Applied Electric Field and Mechanical Boundary Condition on the Stress Distribution at the Crack Tip in Piezoelectric Materials," *Materials Science and Engineering*, Vol. A231, pp. 1~9.

Kwon, J. H., Kwon, S. M., Shin, J. W. and Lee, K. Y., 2000, "Determination of Intensity Factors in Piezoelectric Ceramic Strip with Impermeable Crack," *Transactions of the KSME in Korea*, A, Vol. 24, No. 6, pp. 1601~1607.

Li, C. and Weng, G. J., 2002, "Antiplane Crack Problem in Functionally Graded Piezoelectric Materials," *ASME, Journal of Applied. Mechanics*, Vol. 69, pp. 481~488.

Pak, Y. E., 1990, "Crack Extension Force in a Piezoelectric Materials," *ASME, Journal of Applied. Mechanics*, Vol. 57, pp. 647~653.

Pak, Y. E., 1992, "Linear Electroelastic Fracture Mechanics of Piezoelectric Materials," *International Journal of Fracture*, Vol. 54, pp. 79~100.

Parton, V. Z., 1976, "Fracture Mechanics of Piezoelectric Materials," *Acta Astronautica*, Vol. 3, pp. 671~683.

Shindo, Y., Narita, F. and Tanaka, K., 1996, "Electroelastic Intensification Near Anti-Plane Shear Crack in Orthotropic Piezoelectric Ceramic Strip," *Theoretical and Applied Fracture Mechanics*, Vol. 25, pp. 65~71.

Shindo, Y., Tanaka, K. and Narita, F., 1997, "Singular Stress and Electric Fields of a Piezoelectric Ceramic Strip with a Finite Crack Under Longitudinal Shear," *Acta Mechanica*, Vol. 120, pp. 31~45.

Sosa, H., 1992, "On the Fracture Mechanics of Piezoelectric Solids," *International Journal of Solids and Structures*, Vol. 29, pp. 2613~2622.

Xu, X.-L. and Rajapakse, R. K. N. D., 1999, "Analytical Solution for an Arbitrarily Oriented Void/Crack and Fracture of Piezoceramics," Acta Materialia, Vol. 40, pp. 1735~1747.

Xu, X.-L. and Rajapakse, R. K. N. D., 2001, "On a Plane Crack in Piezoelectric Solids," *International Journal of Solids and Structures*, Vol. 38, pp. 7643~7658.

Zhang, T. Y. and Hack, J. E., 1992, "Mode III Cracks in Piezoelectric Materials," Journal of Applied Physics, Vol. 71, pp. 5865~5870.